Comparative Study on Tetrahedral and Tripodal Luminescent Silane and Methane Compounds with a 2,2′-Dipyridylamino Group

Dong-Ren Bai and Suning Wang*

Department of Chemistry, Queen's University, Kingston, Ontario, K7L 3N6, Canada

Received August 9, 2004

A comparative study on methane and silane derivatives that contain either one or four 2,2′-dipyridylamino group (dpa) functionalized groups has been carried out. Six new compounds, (*p*-dpa-phenyl)triphenylsilane (**1**), (*p*-dpa-phenyl)triphenylmethane (**2**), tetra(*p*-dpa-phenyl)silane (**3**), tetra(*p*-dpa-phenyl)methane (**4**), tetra(*p*-dpa-biphenyl)silane (**5**), and tetra(*p*-dpa-biphenyl)methane (**6**), have been synthesized using Suzuki coupling, Ullmann condensation methods, or simple substitution reactions. The structures of **3** and **4** have been determined by X-ray diffraction analyses. Thermal and luminescent properties have been investigated, which revealed that these new compounds are luminescent in the violet−blue region and the methane derivatives in general have a higher thermal stability than the corresponding silane analogues. The electronic properties of the new compounds were investigated experimentally and theoretically by molecular orbital calculations, which revealed that there is a subtle difference between the methane derivatives and their silane analogues.

Introduction

Luminescent organic and organometallic compounds have attracted much recent attention because of their potential applications in sensor technologies as well as electroluminescent devices.[1−3] Small molecule-based materials have many advantages such as high purity and well-defined structures, compared with polymer-based materials.[4] However, for applications in organic light-emitting diodes (OLEDs), small molecules have the tendency to form crystalline phases in the device, thus destroying film homogeneity and ultimately leading to the instability of the device.[5] It has been well documented that the stability of electroluminescent devices is closely related to the thermal stability of amorphous organic films as measured by glass transition temperatures.[6] Therefore, materials with high glass transition temperature (T_g) and high thermal stability are highly desired for OLED applications. Many different strategies have been explored previously to enhance T_g of molecular compounds. Starburst molecules,[7] dendrimers,[8] and spiro-shaped molecules[9] have been reported to have good film-forming properties with a relatively high T_g. Tetrahedrally shaped molecules based on the methane or silane cores have also been reported to have a high thermal stability and are potentially useful for use in OLEDs.[10] They have also been demonstrated to be very useful building blocks for achieving supramolecular assembly of 3D porous structures.[11] These previous findings have inspired us to investigate luminescent molecules based on a tetrahedral core. The luminescent

(1) (a) Tang, C. W.; Van Slyke, S. A. *Appl. Phys. Lett.* **1987**, *51*, 913. (b) Tang, C. W.; Van Slyke, S. A.; Chen, C. H. J. *Appl. Phys.* **1989**, *65*, 3610. (c) Hu, N.-X.; Esteghamatian, M.; Xie, S.; Popovic, Z.; Ong, B.; Hor, A. M.; Wang, S. *Adv. Mater.* **1999**, *11*, 1460. (d) Bulovic, V.; Gu, G.; Burrows, P. E.; Forrest, S. R.; Thompson, M. E. *Nature* **1996**, *380*, 29. (e) Balzani, V.; Juris, A.; Venturi, M.; Campagna, S.; Serroni, S. *Chem. Rev.* **1996**, *96*, 759. (f) Shen, Z.; Burrows, P. E.; Bulovic, V.; Forrest, S. R.; Thompson, M. E. *Science* **1997**, *276*, 2009. (g) Paplovski, D. B. *Sens. Actuators, B* **1995**, *29*, 213. (h) Ma, Y.; Che, C.-M.; Chao, H.-Y.; Zhou, X.; Chan, W.-H.; Shen, J. *Adv. Mater.* **1999**, *11*, 852. (i) Poterini, G.; Serpone, N.; Bergkamp, M. A.; Netzel, T. L. *J. Am. Chem. Soc.* **1983**, *105*, 4639.

(2) (a) Baldo, M. A.; O'Brien, D. F.; You, Y.; Shoustikov, A.; Sibley, S.; Thompson, M. E.; Forrest, S. R. *Nature* **1998**, *395*, 151. (b) O'Brien, D. F.; Baldo, M. A.; Lamansky, S.; Burrows, P. E.; Thompson, M. E.; Forrest, S. R. *Appl. Phys. Lett.* **1999**, *75*, 4. (c) Lamansky, S.; Djurovich, P.; Murphy, D.; Abdel-Razzag, F.; Kwong, R. C.; Tsyba, I.; Bortz, M.; Mui, B.; Bau, R.; Thompson, M. E. *Inorg. Chem.* **2001**, *40*, 1704. (d) Sprouse, S.; King, K. A.; Spellane, P. J.; Watts, R. J. *J. Am. Chem. Soc.* **1984**, *106*, 6647. (e) Lu, W.; Mi, B. X.; Chan, M. C. W.; Hui, Z.; Zhu, N.; Lee, S. T.; Che, C. M. *Chem. Commun.* **2002**, 206.

(3) (a) Wu, Q.; Esteghamatian, M.; Hu, N.-X.; Popovic, Z.; Enright, G.; Tao, Y.; D'Iorio M.; Wang, S. *Chem. Mater.* **2000**, *12*, 79. (b) Liu, S.-F.; Wu, Q.; Schmider, H. L.; Aziz, H.; Hu, N.-X.; Popovic, Z.; Wang, S. *J. Am. Chem. Soc.* **2000**, *122*, 3671. (c) Wu, Q.; Esteghamatian M.; Hu, N.-X.; Popovic, Z.; Enright, G.; Breeze, S. R.; Wang, S. *Angew. Chem., Int. Ed.* **1999**, *38*, 985. (d) Pang, J.; Tao, Y.; Freiberg, S.; Yang, X.-P.; D'Iorio, M.; Wang, S. *J. Mater. Chem.* **2002**, *12*, 206.

(4) Justel, T.; Nikol, H.; Ronda, C. *Angew. Chem., Int. Ed.* **1998**, *37*, 3084

(5) (a) Han, E.-M.; Do, L.-M.; Niidome, Y.; Fujihura, M. *Chem. Lett.* **1994**, 969. (b) Joswick, M. D.; Cambell, I. H.: Barashkov, N. N.; Ferraris, J. P. *J. Appl. Phys.* **1996**, *80*, 2883.

(6) Tokito, S.; Tanaka, H.; Noda, K.; Okada, A.; Taga, T. *Appl. Phys. Lett.* **1997**, *70*, 1929.

(7) (a) Shirota, Y.; Kobata, T.; Noma, N. *Chem. Lett.* **1989**, 1145. (b) Inada, H.; Shirota, Y. *J. Mater. Chem.* **1993**, *3*, 319. (c) Ueta, E.; Nakano, H.; Shirota, Y. *Chem. Lett.* **1994**, 2397. (d) Inada, H.; Ohnishi, K.; Nomura, S.; Higuchi, A.; Nakano, H.; Shirota, Y. *J. Mater. Chem.* **1994**, *4*, 171. (e) Kageyama, H.; Itano, K.; Ishikawa, W.; Shirota, Y. *J. Mater. Chem.* **1996**, *6*, 675. (f) Tanaka, H.; Tokito, S.; Taga, Y.; Okada, A. *Chem. Commun.* **1996**, 2175. (g) Bettenhausen, J.; Greczmiel, M.; Jandke, M.; Strohriegl, P. *Synth. Met.* **1997**, *91*, 223. (h) O'Brian, D. F.; Burrows, P. E.; Forrest, S. R.; Koene, B. E.; Loy, D. E.; Thompson, M. E. *Adv. Mater.* **1998**, *10*, 1108.

(8) (a) Tanaka, S.; Iso, T.; Doke, Y. *Chem. Commun.* **1997**, 2063. (b) Meier, H.; Lehmann, M. *Angew. Chem., Int. Ed.* **1998**, *37*, 643. (c) Wang, P.-W.; Liu, Y.-J.; Devadoss, C.; Bharathi, P.; Moore, J. S. *Adv. Mater.* **1996**, *8*, 237.

(9) Salbeck, J.; Yu, N.; Bauer, J.; Weissörtel, F.; Bestgen, H. *Synth. Met.* **1997**, *91*, 209.

10.1021/om049382y CCC: $27.50
Publication on Web 11/10/2004

chromophore selected for our investigation is 2,2′-dipyridylamino (dpa), which has been demonstrated by our group to be an efficient and stable fluorescent emitter in the UV−blue region, when attached to an aryl group.[12] Moreover, the dpa group can readily bind to metal ions via the nitrogen donor sites to allow the possible construction of luminescent supramolecular materials via metal−ligand bonds.[12] We report herein the results of our comparative investigation on new silane and methane compounds that are functionalized by either one or four luminescent substituent groups.

Experimental Section

All starting materials were purchased from Aldrich Chemical Co. and were used without further purification. Solvents were freshly distilled over appropriate drying reagents. All experiments were carried out under a dry nitrogen atmosphere by use of standard Schlenk techniques unless otherwise stated. TLC was carried out on silica gel. Flash chromatography was carried out on silica (silica gel 60, 70−230 mesh). ^{1}H and ^{13}C NMR spectra were recorded on Bruker Avance 300, 400, or 500 MHz spectrometers. ^{29}Si NMR spectra were recorded on a Bruker Avance 500 MHz spectrometer. Excitation and emission spectra were recorded on a Photon Technologies International QuantaMaster Model 2 spectrometer. Elemental analyses were performed by Canadian Microanalytical Service Ltd., Delta, British Columbia, Canada. Melting points were determined on a Fisher-Johns melting point apparatus. All DSC measurements were performed on a Perkin-Elmer Pyris DSC 6. Cyclic voltammetry was performed on a BAS CV-50W analyzer with scan rates of 100 mV s^{-1}. The electrolytic cell used was a conventional three-compartment cell, with a Pt working electrode, Pt auxiliary electrode, and Ag/AgCl reference electrode. All experiments were performed at room temperature with 0.10 M tetrabutylammonium hexafluorophosphate in CH_2Cl_2 as the supporting electrolyte. The ferrocenium/ferrocene couple was used as the internal standard. *p*-Dpa-bromobenzene, *p*-dpa-bromo-4,4′-biphenyl, *p*-dpa-phenylboronic acid, and tetra(*p*-bromophenyl)silane[11d] were synthesized by previously reported procedures.[12] Tetra(*p*-bromophenyl)methane and (*p*-iodophenyl)triphenylmethane were synthesized using CPh_3Cl as the starting material according to literature methods.[13] Low-resolution mass spectra were recorded on an Applied Biosystems Voyager DE STR MALDI TOF instrument, and the samples were introduced by laser desorption. High-resolution mass spectra were obtained using electrospray mode with internal calibrants on an Applied Biosystems/MDS-Sciex QSTAR XL spectrometer.

Synthesis of (*p*-Dpa-phenyl)triphenylsilane (1). A hexane solution of *n*-BuLi (1.6 M, 0.68 mL, 1.0 mmol) was added at −78 °C to a solution of *p*-dpa-bromobenzene (0.326 g, 1.0 mmol) in Et_2O (20 mL), and the mixture was stirred for 1 h at that temperature. A solution of triphenyl chlorosilane (0.310 g, 96%, 1.0 mmol) in Et_2O (20 mL) was added to the mixture. The reaction mixture was allowed to reach room temperature over 30 min and stirred overnight. The water layer was separated and extracted with CH_2Cl_2 (3 × 30 mL). The combined organic layers were dried over $MgSO_4$, and the solvents were evaporated under reduced pressure. The residue was subjected to column chromatography on silica gel (ethyl acetate/hexane as eluent) to afford **1** as a pale yellow solid in 35% yield. Mp: 210−212 °C. ^{1}H NMR in $CDCl_3$ (δ, ppm, 25 °C): 8.36 (dd, J = 9.0, 2H), 7.59 (m, 10H), 7.41 (m, 9H), 7.17 (d, J = 8.4 Hz, 2H), 7.03 (d, J = 8.1, 2H), 6.98 (ddd, J = 9.0, 2H). ^{13}C NMR in $CDCl_3$ (δ, ppm, 25 °C): 156.02, 146.62, 144.18, 135.55, 135.53, 134.32, 132.13, 128.12, 127.49, 125.75, 123.35, 116.44, 115.49. ^{29}Si NMR in $CDCl_3$ (δ, ppm, 25 °C): −14.61. MS: *m/z* 505.2 ([M − H]$^+$, 100%, calcd 505.2). Anal. Calcd for $C_{34}H_{27}N_3Si$: C, 80.75: H, 5.38; N, 8.31. Found: C, 80.72; H, 5.45; N, 8.73.

Synthesis of (*p*-Dpa-phenyl)triphenylmethane (2). (*p*-Iodophenyl)triphenylmethane (1.25 mmol, 0.580 g), 2,2′-dipyridylamine (1.33 mmol, 0.150 g), cuprous iodide (0.12 mmol, 0.023 g), 1,10-phenanthroline (0.024 mmol, 0.044 g), and cesium carbonate (2.5 mmol, 0.800 g) were dissolved in 3 mL of DMF. The mixture was heated at 155 °C for 48 h under nitrogen. After cooling to ambient temperature, the reaction mixture was dissolved in 40 mL of CH_2Cl_2 and washed by water. The water layer was separated and extracted with CH_2Cl_2 (3 × 30 mL). The combined organic layers were dried over $MgSO_4$, and the solvents were evaporated under reduced pressure. The residue was subjected to column chromatography on silica gel (ethyl acetate/hexane as eluent) to afford **2** as a colorless solid in 70% yield. Mp: 237−239 °C. ^{1}H NMR in $CDCl_3$ (δ, ppm, 25 °C): 8.38 (d, J = 3.9, 2H), 7.64−7.56 (m, 10H), 7.46−7.37 (m, 9H), 7.18 (d, J = 8.7, 2H), 7.04−6.96 (m, 4H). ^{13}C NMR in $CDCl_3$ (δ, ppm, 25 °C): 158.53, 148.77, 147.27, 143.99, 143.21, 137.83, 132.33, 131.35, 128.00, 126.33, 126.00, 118.65, 117.58, 65.11. MS: *m/z* 488.9 (M$^+$, 100%, calcd. 489.2). Anal. Calcd for $C_{35}H_{27}N_3/0.85H_2O$: C, 83.28: H, 5.35; N, 8.33. Found: C, 82.76; H, 5.65; N, 8.24.

Synthesis of Tetra(*p*-dpa-phenyl)silane (3). A hexane solution of *n*-BuLi (1.6 M, 1.03 mL, 1.65 mmol) was added at −78 °C to a solution of *p*-dpa-bromobenzene (0.490 g, 1.5 mmol) in THF (20 mL), and the mixture was stirred for 1 h at that temperature. A solution of tetraethyl orthosilicate (0.063 g, 0.3 mmol) in THF (10 mL) was added to the mixture. The reaction mixture was stirred for 2 h at −78 °C, allowed slowly to reach room temperature, and stirred overnight. The water layer was separated and extracted with CH_2Cl_2 (3 × 30 mL). The combined organic layers were dried over $MgSO_4$, and the solvents were evaporated under reduced pressure. The residue was subjected to column chromatography on silica gel (THF as eluent) to afford white compound **3** in 36% yield. Compound **3** was recrystallized from CH_2Cl_2/hexane. Mp: 292−294 °C. ^{1}H NMR in CD_2Cl_2 (δ, ppm, 25 °C): 8.32 (dd, J = 4.8, 1.2, 8H), 7.68 (d, J = 8.1, 8H), 7.62 (td, J = 7.8, 1.8, 8H), 7.21 (d, J = 8.1, 8H), 7.06 (d, J = 8.4, 8H), 6.99 (ddd, J = 7.2, 4.8, 1.2, 8H). ^{13}C NMR in $CDCl_3$ (δ, ppm, 25 °C): 158.07, 148.66, 146.28, 137.75, 137.72, 130.38, 125.56, 118.55, 117.59. ^{29}Si NMR in $CDCl_3$ (δ, ppm, 25 °C): −15.27. MS: *m/z* 507.2 ([M + 2H]$^{2+}$, 100%), 1013.3, ([M + H]$^+$, 25%, calcd $C_{64}H_{48}N_{12}Si$, 1012.4). Anal. Calcd for $C_{64}H_{48}N_{12}Si/1CH_2Cl_2$: C, 73.48; H, 4.56; N, 15.31. Found: C, 73.33; H, 5.17; N, 14.83.

Synthesis of Tetra(*p*-dpa-phenyl)methane (4). Tetra(*p*-bromophenyl)methane (0.30 mmol, 0.191 g), 2,2′-dipyridylamine (1.80 mmol, 0.308 g), cuprous iodide (0.12 mmol, 0.023 g), 1,10-phenanthroline (0.024 mmol, 0.044 g), and cesium carbonate (2.50 mmol, 0.800 g) were dissolved in 3 mL of DMF.

(10) (a) Oldham, W. J., Jr.; Lachicotte, R. J. and Bazan, G. C. *J. Am. Chem. Soc*. **1998**, *120*, 2987. (b) Wang, S.; Oldham, W. J., Jr.; Hudack, R. A.; Bazan, G. C. *J. Am. Chem. Soc.* **2000**, *122*, 5695. (c) Robinson, M. R.; Wang, S.; Bazan, G. C.; Cao, Y. *Adv. Mater.* **2000**, *12*, 1701. (d) Aujard, I.; Baltaze, J.-P.; Baudin, J.-B.; Cogne, E.; Ferrage, F.; Jullien, L.; Perez, E.; Prevost, V.; Qian, L.; Ruel, O. *J. Am. Chem. Soc.* **2001**, *123*, 8177. (e) Yeh, H.-C.; Lee, R.-H.; Chan, L.-H.; Lin, T.; Chen, C.-T.; Balasubramaniam, E.; Tao. Y.-T. *Chem. Mater.* **2001**, *13*, 2788. (f) Chan, L.-H.; Lee, R.-H.; Hsieh, C.-F.; Yeh, H.-C.; Chen, C.-T. *J. Am. Chem. Soc.* **2001**, *124*. 6469.

(11) (a) Saied, O.; Maris, T.; Wuest, J. D.; *J. Am. Chem. Soc.* **2003**, *125*, 14956. (b) Brunet, P.; Demers, E.; Maris, T.; Enright, G. D.; Wuest, J. D. A*ngew. Chem. Int. Ed.* **2003**, *42*, 5303. (c) Fournier, J.-H.; Maris, T.; Simard, M.; Wuest, J. D. *Cryst. Growth Des.* **2003**, *3*, 535. (d) Fournier, J.-H.; Maris, T.; Wuest, J. D.; Guo, W.; Galoppini, E. *J. Am. Chem. Soc.* **2003**, *125*, 1002.

(12) (a) Pang, J.; Marcotte, E. J.-P.; Seward, C.; Brown, R. S.; Wang, S. *Angew. Chem., Int. Ed.* **2001**, *40*, 4042. (b) Jia, W.-L.; Liu, Q.-D.; Song, D.; Wang, S. *Organometallics* **2003**, *22*, 321. (c) Seward, C.; Pang, J.; Wang, S. *Eur. J. Inorg. Chem.* **2002**, 1390. (d) Wang, S. *Coord. Chem. Rev.* **2001**, *215*, 79. (e) Yang, W.; Schmider, H.; Wu, Q.; Zhang, Y.; Wang, S. *Inorg. Chem.* **2000**, *39*, 2397.

(13) (a) Su, D.; Menger, F. M. *Tetrahedron Lett.* **1997**, *38*, 1485. (b) Hoskins, B. F.; Robson, R. *J. Am. Chem. Soc.* **1990**, *112*, 1546. (c) Li, Q.; Rukavishnikov, A. V.; Petukhov, P. A.; Zaikova, T. O.; Keana, J. F. W. *Org. Lett.* **2002**, *4*, 3631.

The mixture was heated at 155 °C for 48 h under nitrogen. After cooling to ambient temperature, the reaction mixture was dissolved in 40 mL of CH_2Cl_2 and washed by water. The water layer was separated and extracted with CH_2Cl_2 (3 × 30 mL). The combined organic layers were dried over $MgSO_4$, and the solvents were evaporated under reduced pressure. The residue was subjected to column chromatography on silica gel (ethyl acetate as eluent) to afford pale yellow compound **4** in 25% yield. Mp: >350 °C. ^{1}H NMR in $CDCl_3$ (δ, ppm, 25 °C): 8.41 (d, J = 3.9, 8H), 7.62 (td, J = 1.8, 8.4, 8H), 7.36 (d, J = 8.4, 8H), 7.14 (d, J = 8.4, 8H), 6.99 (m, 16H). ^{13}C NMR in $CDCl_3$ (δ, ppm, 25 °C): 157.85, 148.37, 143.37, 142.65, 137.92, 132.48, 125.63, 118.39, 117.22, 63.85. MS: *m/z* 996.5 (M^+, 100%, calcd. 996.4). HRMS: *m/z*, 997.4192 ($[M + H]^+$, calcd 997.4203).

Synthesis of Tetra(*p*-dpa-biphenyl)silane (5): Method A. A hexane solution of *n*-BuLi (1.6 M, 1.38 mL, 2.2 mmol) was added at −78 °C to a solution of *p*-dpa-bromobiphenyl (0.652 g, 2.0 mmol) in THF (30 mL), and the mixture was stirred for 1 h at that temperature. A solution of $Si(OEt)_4$ (0.092 g, 0.44 mmol) in THF (10 mL) was added to the mixture. The reaction mixture was stirred for 2 h at −78 °C, allowed slowly to reach room temperature, and stirred overnight. The water layer was separated and extracted with CH_2Cl_2 (3 × 30 mL). The combined organic layers were dried over $MgSO_4$, and the solvents were evaporated under reduced pressure. The residue was subjected to column chromatography on silica gel (THF as eluent) to afford white compound **5** in 40% yield. Mp: 280−281 °C.

Method B. To a mixture of *p*-dpa-phenylboronic acid (0.580 g, 2.0 mmol), tetra(*p*-bromophenyl) silane (0.218 g, 0.33 mol), $[Pd(PPh_3)_4]$ (0.073 g, 0.066 mmol), and Na_2CO_3 (1.00 g) was added degassed EtOH (10 mL), H_2O (10 mL), and toluene (20 mL). The mixture was stirred and heated at reflux for 3 days. Following the same workup as in method A, compound **5** was isolated in 75% yield. Mp: 280−282. ^{1}H NMR in CD_2Cl_2 (δ, ppm, 25 °C): 8.43 (d, J = 3.6, 8H), 7.76 (d, J = 8.0, 8H), 7.68 (m, 16H), 7.63 (t, J = 8.0, 8H), 7.30 (d, J = 8.4, 8H), 7.06 (d, J = 8.0, 8H), 6.99 (t, J = 4.8, 8H). ^{13}C NMR in $CDCl_3$ (δ, ppm, 25 °C): 155.95, 146.52, 139.64, 135.78, 135.56, 134.81, 130.70, 126.31, 125.05, 124.42, 124.37, 116.26, 115.11. ^{29}Si NMR in $CDCl_3$ (δ, ppm, 25 °C): −14.43. MS: *m/z* 1316.0 (M^+, 50%, calcd 1316.5). Anal. Calcd for $C_{88}H_{64}N_{12}Si$/1THF: C, 79.54: H, 5.18; N, 12.10. Found: C, 79.87; H, 4.80; N, 11.61.

Synthesis of Tetra(*p*-dpa-biphenyl)methane (6). To a mixture of *p*-dpa-phenylboronic acid (0.320 g, 1.1 mmol), tetra-(*p*-bromophenyl)methane (0.117 g, 0.183mol), $Pd(PPh_3)_4$ (0.055 g, 0.055 mmol), and Na_2CO_3 (1.0 g) was added a mixture of degassed EtOH (6 mL), H_2O (6 mL), and toluene (12 mL). The mixture was stirred and heated at reflux for 3 days. The water layer was separated and extracted with CH_2Cl_2 (3 × 20 mL). The combined organic layers were dried over $MgSO_4$, and the solvents were evaporated under reduced pressure. The residue was recrystallized from CH_2Cl_2 and hexane to afford white compound **6** in 35% yield. Mp: >350 °C. ^{1}H NMR in CD_2Cl_2 (δ, ppm, 25 °C): 8.53 (d, J = 3.6, 8H), 7.71 (d, J = 8.7, 8H), 7.64 (d, J = 8.4, 8H), 7.58 (t, J = 7.5, 8H), 7.43 (d, J = 8.4, 8H), 7.31 (d, J = 8.4, 8H), 6.99 (m, 16H). ^{13}C NMR in $CDCl_3$ (δ, ppm, 25 °C): 158.14, 148.63, 145.69, 144.24, 138.10, 137.64, 137.59, 131.57, 128.22, 127.20, 126.08, 118.30, 117.19, 68.18. MS: *m/z* 1300.1 (M^+, 100%, calcd. 1300.5). Anal. Calcd for $C_{89}H_{64}N_{12}$·0.25CH_2Cl_2: C, 81.05; H, 4.88; N, 12.72. Found: C, 80.86; H, 4.82; N, 12.23.

Photoluminescent Quantum Yield Measurements. Emission quantum yields were determined relative to anthracene in CH_2Cl_2 at 298 K (Φ_r = 0.36). The absorbances of all samples and the standard at the excitation wavelength were approximately 0.096−0.104. The quantum yields were calculated by previously reported procedures.[14]

X-ray Crystallographic Analysis. Single crystals of **3** were obtained from solution of $CHCl_3$ and **4** from solution of ethyl acetate. All crystals were mounted on glass fibers for data collection. Data were collected on a Siemens P4 single-crystal X-ray diffractometer with a CCD-1000 detector and graphite-monochromated Mo Kα radiation, operating at 50 kV and 30 mA. All data collection was carried out at ambient temperature. The 2θ data collection ranges are 3.00−57.00° for all compounds. No significant decay was observed in any samples. Data were processed on a PC with the aid of the Bruker SHELXTL software package (version 5.10) and are corrected for absorption effects. All structures were solved by direct methods. Disordered $CHCl_3$ solvent molecules are located in the crystal lattices of **3**. All non-hydrogen atoms except those on some of the disordered solvent molecules were refined anisotropically. The positions of hydrogen atoms were either located directly from difference Fourier maps or calculated and their contributions in structural factor calculations were included.

Scheme 1

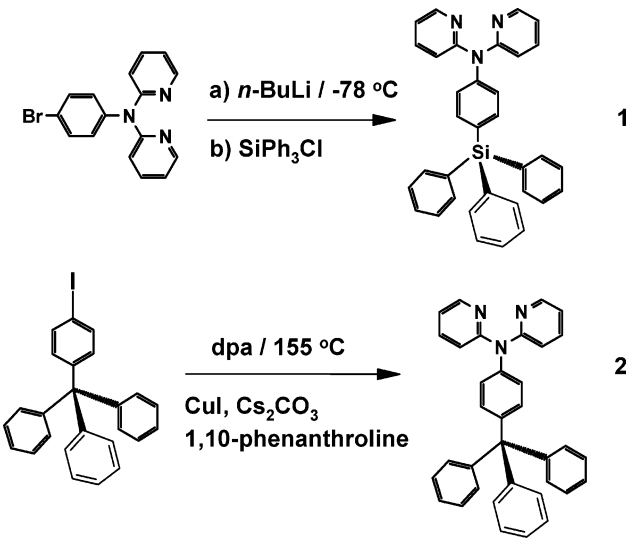

Results and Discussion

Syntheses. The syntheses of compounds **1**−**6** were achieved by either direct substitution, or Suzuki coupling, or Ullmann condensation methods. The syntheses of the two tripodal compounds **1** and **2** are illustrated in Scheme 1. Compound **1** contains one functionalized phenyl group and was obtained by the one-step substitution reaction of Li-4-dpa-phenyl with $SiPh_3Cl$ in 35% yield. Its carbon analogue, compound **2**, was obtained by Ullmann condensation reaction between CPh_3(4-I-Ph) and 2,2′-dipyridylamine catalyzed[15] by copper(I) in the presence of 1,10-phenanthroline and cesium carbonate in ∼70% yield. The synthetic procedures for the tetrahedral silicon and carbon compounds **3** and **4** are shown in Scheme 2. Compound **3** contains four functionalized phenyl groups and was obtained by a substitution reaction between Li-4-dpa-phenyl and $Si(OEt)_4$ in 36% yield. The tetrahedral carbon analogue, compound **4**, was obtained by an Ullmann condensation reaction between C(4-Br-Ph)$_4$ and 2,2′-dipyridylamine catalyzed by copper(I) in the presence of 1,10-phenanthroline and cesium carbonate in 25% yield. Not sur-

(14) (a) Demas, N. J.; Crosby, G. A. *J. Am. Chem. Soc.* **1970**, *29*, 7262. (b) Berlman, I. B. *Handbook of Fluorescence Spectra of Aromatic Molecules*; Academic Press: New York, 1971.

(15) Klapars, A.; Antilla, J. C.; Huang, X.; Buchwald, S. L. *J. Am. Chem. Soc.* **2001,** *123*, 7727.

Scheme 2

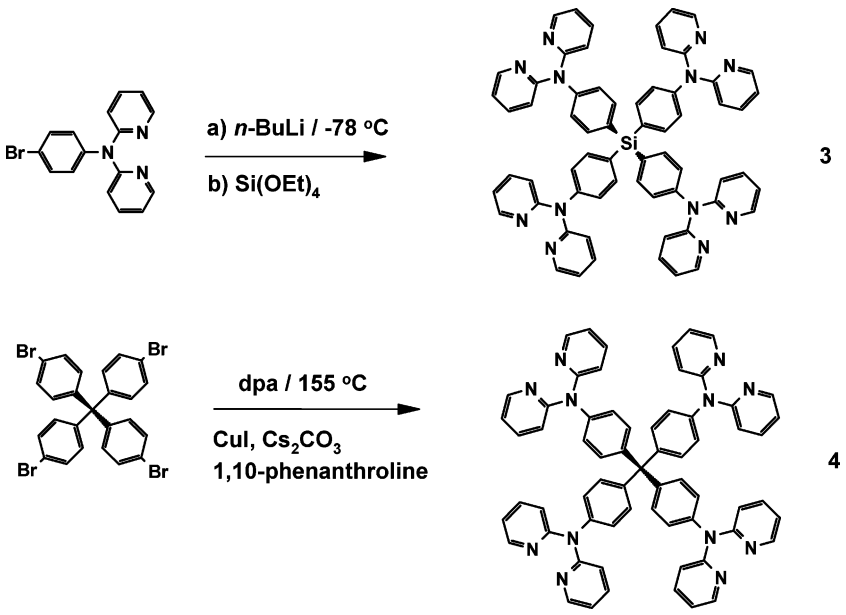

Scheme 3

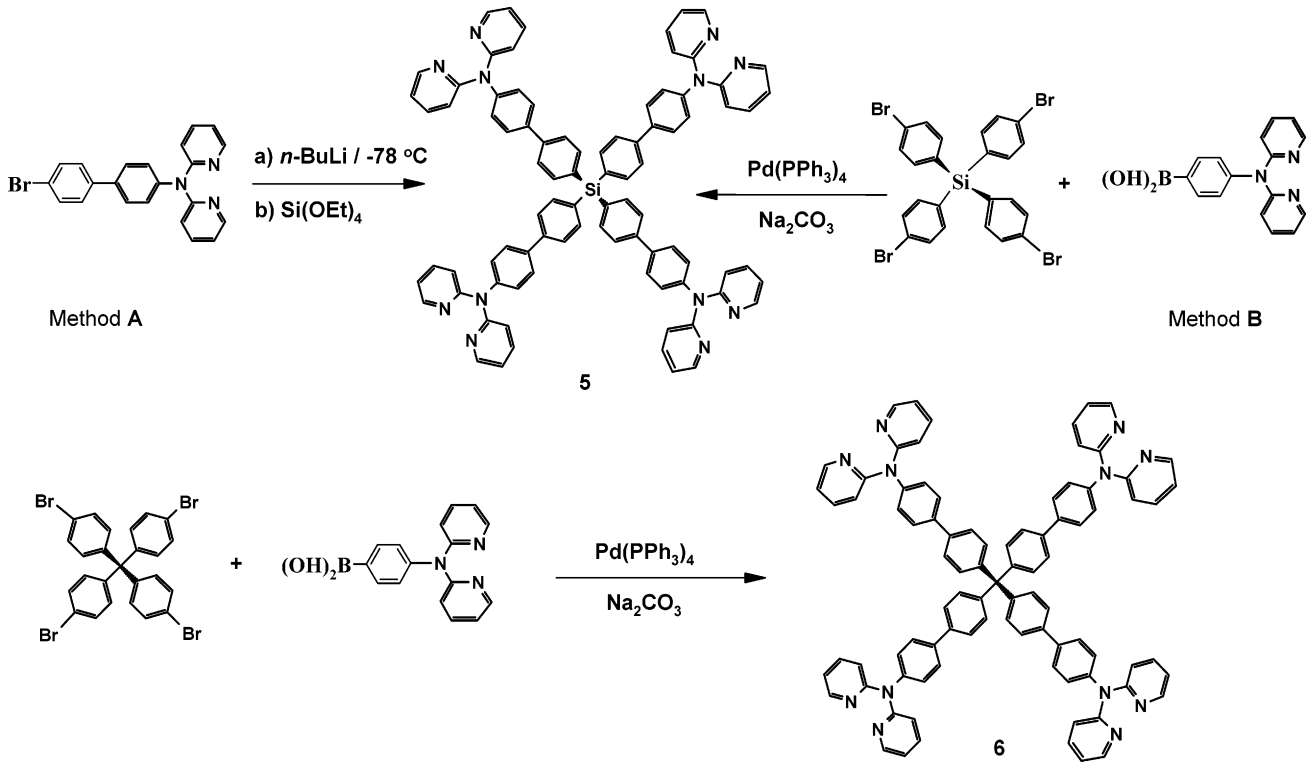

prisingly, the Ullmann condensation for **4** that involves four substituent groups gave a much lower yield than the Ullmann condensation for **2** that involves only one substituent, as substantial amount of trisubstituted product was identified. The tetrahedral silicon compound **5** that contains four functionalized 4,4′-biphenyl groups can be obtained by two different approaches, A and B, as shown in Scheme 3. In method A, compound **5** was obtained by the substitution reaction between Li-*p*-dpa-biphenyl and $Si(OEt)_4$ in 40% yield in the same manner as for compound **3**. In method B, **5** was obtained by a Suzuki cross-coupling reaction[16] between Si(4-Br-Ph)$_4$ with *p*-dpa-phenylboronic acid in the presence of Na_2CO_3 as a base and using $Pd(PPh_3)_4$ as the catalyst in 75% yield. Clearly the Pd-catalyzed Suzuki coupling reaction produces compound **5** in a much higher yield than the substitution reaction. However, method B does involve an extra synthetic step, i.e., the synthesis of the starting material Si(4-Br-Ph)$_4$, compared to method A. On the other hand, method A, albeit one step simpler, has the tendency to produce multiple products. For example, even if a six-to-one ratio (four-to-one theoretically) of the two starting materials was used in the synthesis of **5** using method A, the presence of trisubstituted product was always observed, which, with a

(16) (a) Miyaura, N. *Adv. Met.-Org. Chem.* **1998**, *6*, 187, and references therein. (b) Suzuki, A. *J. Organomet. Chem.* **1999**, *576*, 147, and references therein. Links.

Table 1. Crystal Data for 3 and 4

	3	4
formula	$C_{64}H_{48}N_{12}Si/8CHCl_3$	$C_{65}H_{48}N_{12}$
fw	1968.18	997.16
T (K)	298	296
space group	I_1/a	$P4_2/n$
a [Å]	25.5779(17)	14.558(3)
b [Å]	25.5779(17)	14.558(3)
c [Å]	13.7775(14)	11.723(4)
α [deg]	90	90
β [deg]	90	90
γ [deg]	90	90
V [Å^3]	9013.6(12)	2484.7(11)
Z	4	2
d_{calcd} [g cm^{-3}]	1.450	1.333
μ [mm^{-1}]	0.785	0.082
$2\theta_{max}$ [deg]	46.70	56.76
no. of reflns measd	22 519	11 886
no. of reflns used (R_{int})	3260 (0.0656)	2993 (0.0427)
no. of params	277	174
final R ($I>2\sigma(I)$)		
R_1[a]	0.0625	0.0596
wR_2[b]	0.1671	0.1657
R (all data)		
R_1[a]	0.1266	0.1398
wR_2[b]	0.1913	0.2008
goodness of fit on F^2	0.876	0.879

[a] $R_1 = \sum[|F_o| - |F_c|]/\sum|F_o|$. [b] $wR_2 = \{\sum[w(F_o^2 - F_c^2)]/\sum(wF_o^2)\}^{1/2}$. $w = 1/[\sigma^2(F_o^2) + (0.075P)^2]$, where $P = [\max(F_o^2,0) + 2F_c^2]/3$.

Table 2. Selected Bond Lengths (Å) and Angles (deg) for 3 and 4

		Compound **3**	
Si(1)−C(1)	1.869(4)	C(1)−Si(1)−C(1′)	111.34(12)
C(4)−N(1)	1.420(5)	C(1)−Si(1)−C(1″)	105.8(2)
C(7)−N(1)	1.411(5)	C(4)−N(1)−C(7)	119.0(3)
C(12)−N(1)	1.409(5)	C(4)−N(1)−C(12)	119.9(3)
		C(7)−N(1)−C(12)	120.8(3)
		Compound **4**	
C(1)−C(2)	1.528(2)	C(2)−C(1)−C(2′)	111.85(8)
C(5)−N(1)	1.440(3)	C(2)−C(1)−C(2″)	104.80(16)
C(8)−N(1)	1.339(3)	C(5)−N(1)−C(8)	121.0(2)
C(13)−N(1)	1.403(3)	C(5)−N(1)−C(13)	116.5(2)
		C(8)−N(1)−C(13)	122.5(2)

polarity quite similar to the four-substituted product, made the separation and purification process very difficult. Therefore, we believe that method B is overall better for the synthesis of compound **5** in terms of yield and ease of purification and separation. The carbon analogue of **5**, compound **6**, was obtained by a Suzuki coupling method B similar to that used for **5**. The reaction between C(4-Br-Ph)$_4$ and *p*-dpa-phenylboronic acid in the presence of Na_2CO_3 as a base and Pd(PPh$_3$)$_4$ as the catalyst produced **6** in 30% yield. The relatively low yield of **6** may be attributed to the smaller size of carbon atom, compared to silicon, which imposes a greater steric hindrance. Also, the use of the relatively inefficient Pd(PPh$_3$)$_4$ catalyst may be another contributing factor.[10b] Compounds **1**−**6** were fully characterized by NMR, mass spectroscopy, and elemental analyses. The structures of **3** and **4** were determined by single-crystal X-ray diffraction analyses.

Crystal Structures of 3 and 4. Crystal data of **3** and **4** are provided in Table 1. Selected bond lengths and angles for these two compounds are provided in Table 2. Both molecules possess a crystallographically imposed $S\bar{4}$ symmetry. The structures of **3** and **4** are shown in Figure 1. The central silicon atom in **3** and the central carbon atom in **4** adopt a typical tetrahedral geometry surrounded by four carbon atoms. The Si−C

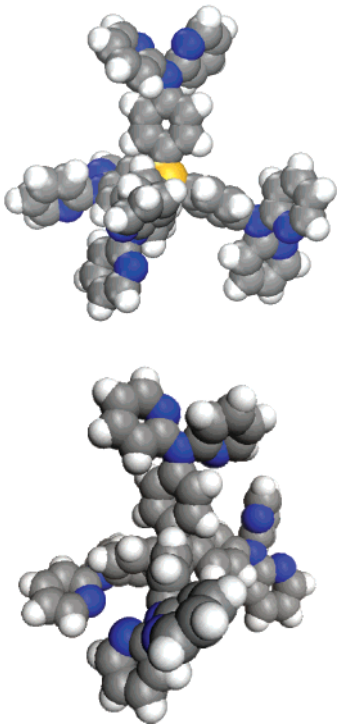

Figure 1. Molecular structures of **3** (top) and **4** (bottom) shown as space-filling diagrams.

(phenyl) bond length in **3** is similar to those of previously reported phenylsilane derivatives.[12b] The C−C (phenyl) bond length in **4** is typical for single C−C bonds. The amino nitrogen atom on the PhNPy$_2$ ligand in both structures is essentially coplanar with the three bound carbon atoms, which have a trigonal planar geometry. Although the C−N (amino) bond lengths of **3** and **4** are similar to those of previously reported dpa derivatives,[12] there is a subtle difference in the two structures. The C−N (amino) bond lengths in **3** are quite uniform (1.409(5)−1.420(5) Å), but in contrast, there is a considerable variation of the C−N (amino) bond lengths in **4** (1.339(3)−1.440(3) Å). The pyridyl rings are not coplanar with the phenyl ring in both structures, as shown by Figure 1. Instead, the two pyridyl rings of the dpa group are oriented above and below the phenyl ring, respectively. This lack of coplanarity is clearly caused by the *ortho*-hydrogen steric interactions imposed by two pyridyl rings on the central phenyl ring. Chloroform solvent molecules were located inside the lattice of **3** (8 $CHCl_3$ per molecule of **3**). The C−C−C angles at the core of **4** have values of either 104.80° or 111.85°, whereas the C−Si−C angles at the core of **3** vary less widely (105.9° or 111.28°), despite the presumably greater flexibility of the silicon core. The same trend was also observed in some methane and silane derivatives reported recently.[11d] One interesting and important feature for both structures is that both molecules are arranged in such a manner in the crystal lattice that the pyridyl groups from neighboring molecules form a one-dimensional square channel (Figures 2 and 3). The shortest intermolecular contact among the pyridyl groups that form the square channel is between N(2) and C(9′) (3.51 Å). A weak hydrogen-bonding interaction between N(2) and H(9A′)−C(9′) is likely present. The dimensions of the square channel in the lattice of **3** (∼5.72 × 5.72 Å) are much greater than those in the lattice of **4** (3.56 ×

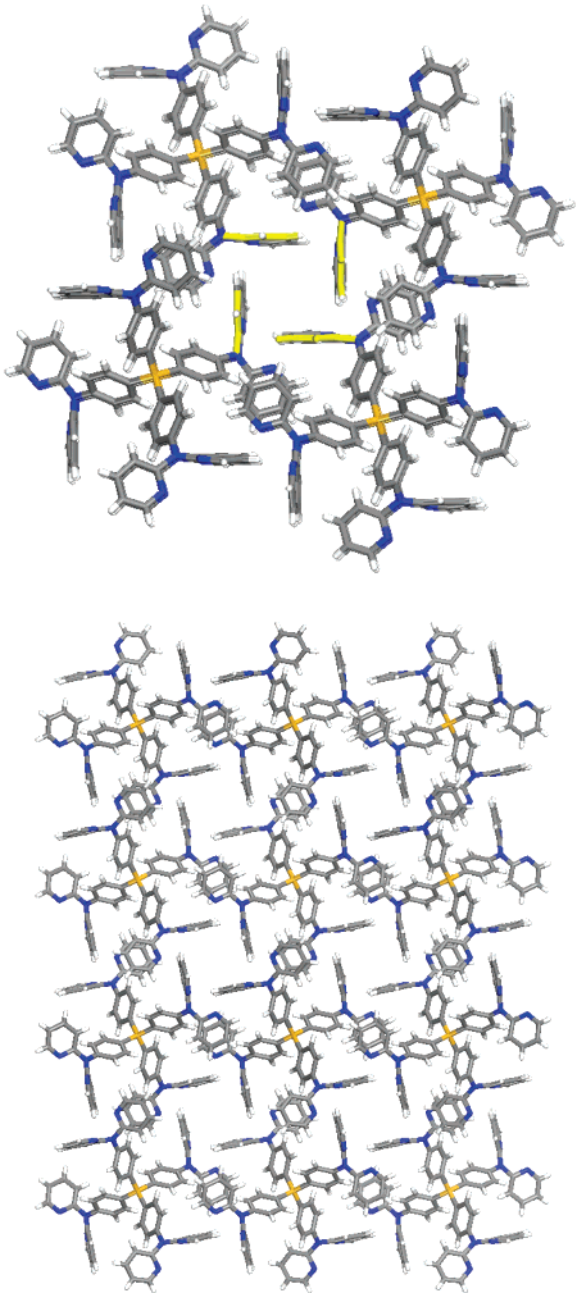

Figure 2. Packing diagrams showing the single square channel (top) and the multiple square channels in the crystal lattice of **3**. The $CHCl_3$ solvents were omitted for clarity.

3.56 Å). Perhaps, as a result, the crystal lattice of **3** is capable of trapping solvent molecules such as $CHCl_3$, while no solvent molecules were located in the lattice of **4**. Some $\pi-\pi$ stacking interaction is evident in **4**, as indicated by the shortest interplane separation distance of 3.56 Å between two pyridyl groups of neighboring molecules (see Supporting Information).

Single crystals of **5** and **6** suitable for X-ray diffraction study could not be obtained. Nonetheless, elemental analyses indicated that the silane compound **5** cocrystallizes with THF solvent molecules (1 THF per molecule of **5**), while the methane compound **6** has no solvents in the crystal lattices. This is further confirmed by TGA experiments, which showed that compound **5** is stable up to 290 °C and ~5% weight was lost from 70 °C to 260 °C, consistent with the loss of THF solvent molecules trapped in the solid.

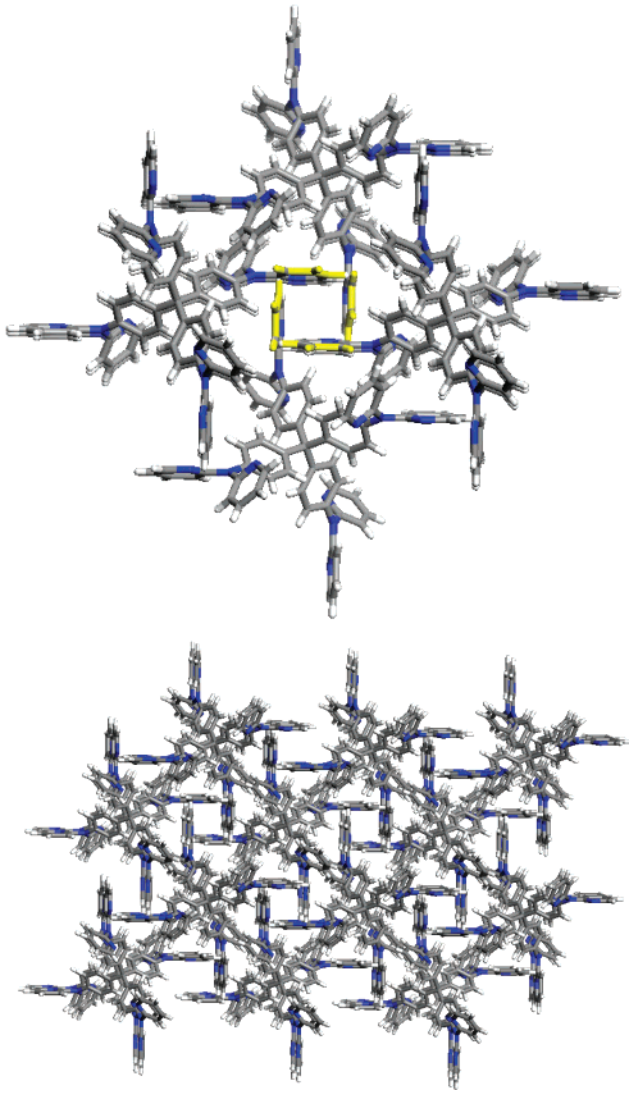

Figure 3. Packing diagrams showing the single square channel (top) and the multiple square channels in the crystal lattice of **4**.

Table 3. Thermal Properties of 1−6 from DSC Measurements[a]

compound	T_g (°C)	T_c (°C)	T_m (°C)
1	50	153	210
2	74	165	237
3	100	185	292
4	n/a	n/a	>350
5	140	150	280
6	155	n/a	>350

[a] Heating rate = 10 °C/min cooling rate = 20 °C/min.

Physical Properties. The six new compounds are stable in solution and in the solid state upon extended exposure to air. These compounds also exhibit remarkable thermal stability as shown in Table 3, with melting points ranging from 210 °C (**1**) to >350 °C (**4** and **6**). Perhaps one of the most significant differences between the silane compounds **1**, **3**, and **5** and their methane analogues **2**, **4**, and **6** is the thermal stability. As shown in Table 3, the silane compounds all display a lower melting point than the corresponding methane analogues. A similar trend was also observed in silicon- and

Table 4. HOMO and LUMO Energy of Compounds 1−6

compound	HOMO (eV)	LUMO (eV)	experimental energy gap (eV)	HOMO from MO calculation	LUMO from MO calculation	band gap from MO calculation
1	−5.78	−2.22	3.56	−5.5312	−0.9853	4.5459
2	−5.70	−2.21	3.49	−5.2409	−0.5589	4.6820
3	−5.78	−2.26	3.52	−5.5379	−1.1028	4.4351
4	n/a	n/a	3.44	−5.0190	−0.4653	4.5537
5	−5.65	−2.21	3.44	n/a	n/a	n/a
6	−5.63	−2.24	3.39	n/a	n/a	n/a

carbon-based tetrahedral molecules reported previously by Bazan et al.[10b] DSC experiments indicate all but compound **4** are capable of forming amorphous phases. There are two general trends observed for these molecules. First, the methane molecules in general display higher T_g than the corresponding silane analogues. For example, the silanes **1** and **5** have a T_g of 50 and 140 °C, respectively while the methane analogues **2** and **6** have a T_g of 74 and 155 °C, respectively. The relatively high T_g of the methane derivatives may be due to the presence of stronger intermolecular interactions as revealed by the crystal structures of **3** and **4**. Second, the tripodal molecules have a lower T_g than those of the tetrahedral molecules, and among the tetrahedral molecules, the dpa-functionalized tetraphenyl silane or methane has a much lower T_g (e.g., **3**, 100 °C) than that of the dpa-functionalized tetra-biphenylsilane or methane (e.g., **5**, 150 °C). The fact that tetrahedral molecules exhibit much higher T_g than the tripodal molecules could be interpreted by the relatively high molecular weight and the larger size of the tetrahedral molecules. The extension in conjugation length in **5** relative to **3** that results in an increase of 40 °C in T_g is consistent with the previous observation on silane and methane analogue molecules by Bazan et al.[10b] The high thermal stability and high glass transition temperature displayed by compounds **1**−**6** are comparable to the behavior of our previously reported dpa-functionalized triangular starburst molecules based on either a triphenylbenzene core or a triphenyl-triazine core.[3d]

Electronic Properties. The UV−vis spectra of compounds **1**−**6** all exhibit two intense absorption bands with λ_{max} at ∼230 nm and 300−316 nm, respectively, which can be attributed to the $\pi-\pi^*$ transitions involving the phenyl/biphenyl and the dpa group. The oxidation potentials for compounds **1**−**3** and **5/6** were obtained by cyclic voltammetry measurements in CH_2Cl_2, which established the HOMO levels for these compounds. Because we could not obtain the reduction potentials for compounds **1**−**6**, the LUMO levels for all compounds were calculated from the experimentally measured HOMO levels and the energy gaps estimated from the absorption edge in the UV−vis spectra. Due to the poor solubility of compound **4**, no oxidation or reduction potential was obtained. The data are summarized in Table 4. One interesting observation is that the silane molecules have HOMO and LUMO levels almost identical to those of the corresponding methane analogues (although the silane molecules have a slightly bigger HOMO−LUMO gap than the methane analogues), an indication that the replacement of the silicon atom by a carbon atom in the center of the tetrahedron does not have significant impact on the electronic properties of the molecule. The electronic level in **1**−**6** appears to be dictated by the dpa-functionalized aryl group. For example, the silane compounds **1** and **3** contain the same dpa-phenyl group and have similar HOMO and LUMO levels. In contrast, the HOMO level (−5.65 eV) of the silane compound **5** is above that of **1** and **3** (−5.78 eV), which is clearly caused by the presence of the biphenyl group in **5**, which effectively increases the conjugation length, thus pushing the HOMO level higher.

Luminescence. Compounds **1**−**6** emit a violet to blue color in solution and in the solid state when irradiated by UV light. The fluorescence spectra observed for **3**−**5** in CH_2Cl_2 solution are shown in Figure 4 as representative examples. The λ_{max} of emission in solution for **1**−**6** ranges from 378 nm (**1**) to 397 nm (**4**). For the silane compounds, the emission energy in solution shows a slight red shift from the tripodal molecule **1** to the biphenyl tetrahedral molecule **5**. The extension of the phenyl linker in **3** to the biphenyl linker in **5** causes a red shift of 9 nm, due to again the increased conjugation. For the methane derivatives, the emission energy in solution does not show drastic change from the tripodal **2** to the biphenyl tetrahedral **6**, as shown by Table 5. Interestingly however, the methane derivatives appear to emit at a somewhat longer wavelength than the corresponding silane analogues. Compounds **1**−**6** are all fairly efficient emitters in solution, as indicated by their quantum efficiency. No obvious trend in the quantum efficiency was observed. In the solid state, the emission maximum of **1**−**6** is considerably red shifted, compared to that in solution (Table 5 and Figure 5), which is likely caused by intermolecular $\pi-\pi$ stacking interactions in the solid state as displayed by compound **4** in the solid state. The relatively large band gaps displayed by compounds **3**−**6** and their relatively high quantum

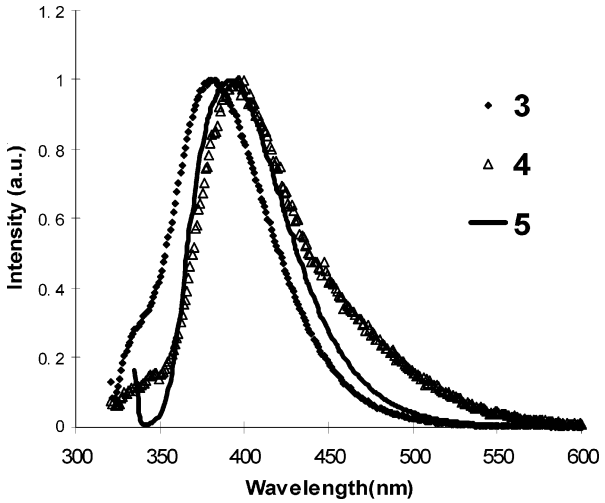

Figure 4. Emission spectra of **3**−**5** in CH_2Cl_2. The spectrum of **1** is similar to that of **3**, and the spectra of **2** and **6** are similar to that of **5**. They are therefore omitted for clarity.

Table 5. Luminescent Data

compound	UV−vis absorption (nm)	excitation (nm)	emission (nm)	quantum yield (%)	conditions (298 K)
1	230, 304	310	378	12	CH_2Cl_2
		326	401		solid state
2	230, 300	303	393	43	CH_2Cl_2
		372	448		solid state
3	230, 304	307	381	9	CH_2Cl_2
		361	400		solid state
4	230, 302	307	397	8	CH_2Cl_2
		354	437		solid state
5	230, 314	324	390	48	CH_2Cl_2
		370	403		solid state
6	230, 316	321	390	16	CH_2Cl_2
		366	397		solid state

efficiency along with their high T_g's make them potentially useful as either a hosting material for emitters or a hole or electron blocking layer in electroluminescent devices.[17]

Molecular Orbital Calculations. To gain a deeper insight into the electronic and luminescent properties of compounds **1**−**6**, we performed ab initio molecular orbital calculations on compounds **1**−**4**. Crystal structure geometric parameters were used for the calculations for compounds **3** and **4**, while molecular modeling and geometric optimization were carried out to obtain geometric parameters required by the calculation for compound **1** and **2**. The Gaussian suite of programs[18] (Gaussian 98) was employed for the calculations. The calculations were performed with the 6-31G* basis set[9] for compounds **2** and **4** and the 6-311G** basis set for compounds **1** and **3** at the RHF (restricted Hartree−Fock) level of computation. The orbital diagrams were generated by use of the Molekel program.[20] All contour values are ±0.025 au. The calculated HOMO and LUMO energy levels and band gaps for **1**−**4** are provided in Table 4. The results of MO calculations showed that the HOMO and LUMO levels are π and π^* orbitals involving the dpa-functionalized phenyl group. The trend of the calculated HOMO and LUMO levels for **1**−**4** is consistent with that determined experimentally. One feature that is not very obvious experimentally is that the methane molecules **2** and **4** have a higher HOMO and a higher LUMO level, relative to those of the corresponding silane molecules **1** and **3**.

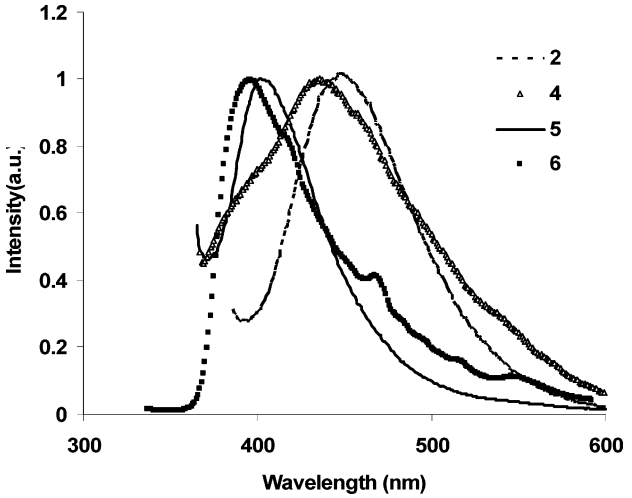

Figure 5. Emission spectra of **2** and **4**−**6** in the solid state. The spectra of **1** and **3** are similar to those of **5** and **6** and are therefore not shown for clarity.

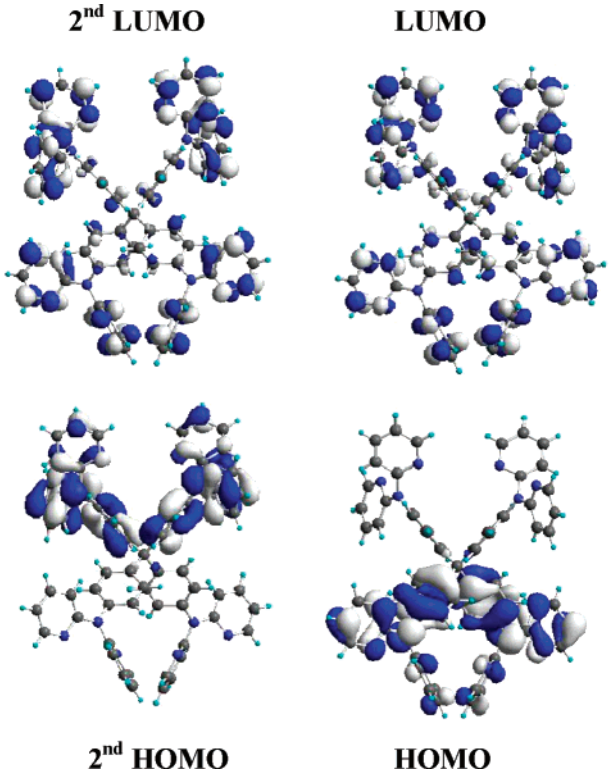

Figure 6. Orbital diagrams for HOMO, second HOMO, LUMO, and second LUMO levels of compound **4**.

This appears to support that the silicon atom can somewhat stabilize both HOMO and LUMO levels, compared to the carbon analogues. In addition, the calculated band gaps for the methane derivatives are also somewhat smaller than those of the silane analogues, which is consistent with the experimentally observed trend and the fact that the methane derivatives have a relatively longer emission wavelength. As an example, the HOMO, second HOMO, LUMO, and second LUMO levels for **4** are shown in Figure 6. Due to the presence of molecular symmetry in **4**, the HOMO and second HOMO levels are in fact degenerated. On the basis of the MO calculation results, the observed electronic transitions and luminescence for compounds **1**−**6** can be assigned to π−π^* transitions.

Conclusions

Three dpa-functionalized phenyl and biphenylsilane compounds and their methane analogues have been

(17) (a) Tsutsui, T. *Mater. Res. Soc. Bull.* **1997**, June, 39. (b) Chen, C. J.; Shi, J. *Coord. Chem. Rev.* **1998**, *171*, 161. (c) Mitschke, J.; Bauerle, P. *J. Mater. Chem.* **2000**, *10*, 1471. (d) Shirota, Y. *J. Mater. Chem.* **2000**, *10*, 1.

(18) Frisch, M. J.; Trucks, G. W.; Schlegel, H. B.; Scuseria, G. E.; Robb, M. A.; Cheeseman, J. R.; Zakrzewski, V. G.; Montgomery, J. A., Jr.; Stratmann, R. E.; Burant, J. C.; Dapprich, S.; Millam, J. M.; Daniels, A. D.; Kudin, K. N.; Strain, M. C.; Farkas, O.; Tomasi, J.; Barone, V.; Cossi, M.; Cammi, R.; Mennucci, B.; Pomelli, C.; Adamo, C.; Clifford, S.; Ochterski, J.; Petersson, G. A.; Ayala, P. Y.; Cui, Q.; Morokuma, K.; Malick, D. K.; Rabuck, A. D.; Raghavachari, K.; Foresman, J. B.; Cioslowski, J.; Ortiz, J. V.; Stefanov, B. B.; Liu, G.; Liashenko, A.; Piskorz, P.; Komaromi, I.; Gomperts, R.; Martin, R. L.; Fox, D. J.; Keith, T.; Al-Laham, M. A.; Peng, C. Y.; Nanayakkara, A.; Gonzalez, C.; Challacombe, M.; Gill, P. M. W.; Johnson, B. G.; Chen, W.; Wong, M. W.; Andres, J. L.; Head-Gordon, M.; Replogle, E. S.; Pople, J. A. *Gaussian 98*, revision A.6; Gaussian, Inc.: Pittsburgh, PA, 1998.

(19) Wong, D. E.; Dunning, T. H.. Jr. *J. Chem. Phys.* **1993**, *98*, 1358.

(20) Flkiger, P.; Lthi, H. P.; Portmann, S.; Weber, J. *MOLEKEL 4.1*; Swiss Center for Scientific Computing: Manno, Switzerland, 2000−2001.

synthesized. A comparative study on structural, thermal, and electronic properties of these two series of compounds has been conducted. Both tetrahedral silane and methane compounds have the tendency to crystallize in tetragonal space groups and form tetragonal 1D channels in the crystal lattice. The silane compound has the tendency to trap solvent molecules in the lattice, while the methane compound does not, as demonstrated by compounds **3**−**6**, which may be attributed to the longer Si−C bonds and the resulting larger cavity of the extended channel, compared to the methane molecules. Perhaps as a consequence of a tighter lattice packing and stronger intermolecular interactions (as shown by the structures of **3** and **4**), the methane molecules in general have a higher thermal stability, as reflected by their T_g and T_m, than their silane analogues. The thermal stability of the silane or methane series appears to increase with the increase of the number of substituent groups and the size of the molecule. Electronically there is a subtle difference between the methane molecules and the silane analogues: the band gap of the former is slightly smaller than that of the latter. MO calculations support that the silicon atom in silane appears to stabilize both HOMO and LUMO levels, compared to the carbon atom in methane, and that the observed electronic transitions of the new compounds are due to $\pi-\pi^*$ transitions. The new silane and methane compounds are fairly efficient emitters in the violet−blue region. For some of the new molecules, the combination of their high thermal stability and their large HOMO−LUMO band gap make them potentially useful candidates as either hosting materials or charge-blocking layers in OLEDs. Our preliminary investigation indicated that the tripodal and tetrahedral silane and methane molecules are useful building blocks for the construction of extended supramolecular networks via the formation of coordination bonds at the 2,2′-dipyridylamino sites. A full account on the utilities of these new molecules in supramolecular assembly will be reported in due course.

Acknowledgment. We thank the Natural Sciences and Engineering Research Council of Canada for financial support.

Supporting Information Available: Complete listing of crystal data for **3** and **4**, including complete drawings with labeling schemes, tables of atomic coordinates, thermal parameters, bond lengths and angles, and hydrogen parameters, and a drawing showing $\pi-\pi$ stacking interaction in the crystal lattice of **4**. This material is available free of charge via the Internet at http://pubs.acs.org.

OM049382Y